COMPUTATION OF A DOUBLE-SIDED LINEAR INDUCTION MOTOR BY UNDAMPED TRAVELING WAVES

By

GY. TEVAN

Institute of Heavy Current Engineering, Technical University, Budapest

Received April 18, 1979
Presented by Prof. Dr. GY. RETTER

1. Introduction

A crucial problem in computing linear induction motors is the treatment of end-effect. From this aspect, relevant publications belong to two groups, concerning either

a) purely undamped, or

b) damped

traveling waves.

A single undamped traveling wave only suits the computation of linear motors of "infinite length" [6, 8, 12, 13]. A Fourier integral yields an "infinity" of undamped traveling waves [3, 9], to the detriment of ease of computation and understanding. Also the three-dimensional model by Oberretl [10] applying undamped traveling waves, uses Fourier series expansion to compose the solution from discreet traveling waves, offering a rather high accuracy; the multitude of traveling waves, however, require to draw even general conclusions by means of a computer.

Recently, YAMAMURA [7, 15, 17], VOLDEK [5, 14] and al. stressed damped traveling field models; their surveyability and evaluability prevail in the one-dimensional mode of discussion. The description involving damped waves has the shortcomings of being not related any more to the theory of rotating induction motor, and of difficulties in the complex correct handling of the end and edge effects; namely the edge effect is best determined according to BOLTON [4] referring to undamped traveling waves.

In what follows, analysis of the excitation pattern will be involved to approximate reality by means of some, in part fraction-order, undamped traveling fields. The presented algorithm reckons with all essential effects, theoretically founded but with certain simplifications for the sake of comprehensiveness. It also suits general conclusions and rapid calculation.

2. Analysis of the excitation pattern

Electromagnetic field inside a confined space part is known to be determinable in possession of the tangential component of electric or magnetic field intensity (or linear combination of both) on the boundary surfaces at any instant. To determine the electromagnetic field in the air gap and secondary part of the linear induction motor, distribution of the tangential component of magnetic field intensity on the boundary surface of the primary part is considered, independent (at a close approximation) of the motor load and rather simple to compute from the primary excitation.

Analysing first the case of the "infinite" primary part, the scheme in Fig. 1 is the distribution of H_z at the excitation of a single phase, where there is $q=1$ slot for each phase and pole; z being the coordinate along the travel, τ_p the pole pitch, c the slot-opening, and Θ the excitation share on one slot. (Tangential component of magnetic field intensity on the iron surface is negligible, while along the slot surface it may be considered as of about uniform distribution supposed, that the slot-opening is sufficiently sinall.)

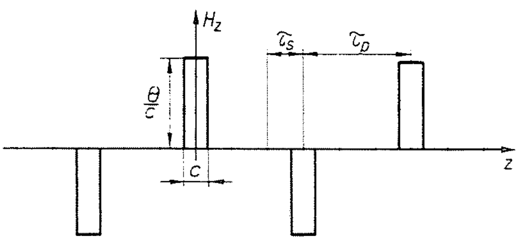

Fig. 1

In the Fourier series of the periodic distribution seen in Fig. 1, only the amplitudes of cosine terms of odd order $\nu=1+2k$ $(k=0, 1, 2, \ldots)$ are non-zero, viz.:

$$H_{z\nu}^{(f)}=\frac{2\Theta}{\tau_p}\frac{\sin\left(\nu\frac{\pi}{\tau_p}\frac{c}{2}\right)}{\nu\frac{\pi}{\tau_p}\frac{c}{2}}$$

For $q>1$, the amplitude of the ν-th harmonic decreases according to a distribution factor

$$\frac{\sin\left(\nu\frac{\pi}{6}\right)}{q\,\sin\left(\nu\frac{\pi}{6q}\right)}$$

compared to the q-fold value.

Thus, in the general case, excitation of one phase causes the νth harmonic to have an amplitude:

$$H_{z\nu}^{(f)}=\frac{2\Theta}{\tau_p}q\xi_\nu \tag{1}$$

where:

$$\xi_\nu=\frac{\sin\left(\nu\frac{\pi}{\tau_p}\frac{c}{2}\right)}{\nu\frac{\pi}{\tau_p}\frac{c}{2}}\,\frac{\sin\left(\nu\frac{\pi}{6}\right)}{q\,\sin\left(\nu\frac{\pi}{6q}\right)} \tag{2}$$

Feeding the phase winding by sine A. C. results in standing waves for any harmonic, that can be decomposed in the usual manner into sums of half-amplitude waves traveling in opposite directions. Feeding the phase windings by a three-phase, symmetric current system, in case of $\nu=6k+1$ all but positive-order traveling waves and of negative order for $\nu=6k-1$ are excluded from the resultant, while for $\nu=3k$ the resultant becomes zero. Since the three half-amplitude traveling waves remaining in the resultant for $\nu=6k+1$ are in phase, the amplitude of the νth harmonic wave resultant, using Eq. (1) becomes:

$$H_\nu=\frac{3}{2}H_{z\nu}^{(f)}=\frac{3\Theta}{\tau_p}q\xi_\nu \tag{3}$$

Analysis of the finite primary part will start with the case of slots fully wound even at edges. In case of windings of finite length, distributions $H_z(z)$ excited by one phase winding are zero outside the extreme slots belonging to the given phase. Expanding these functions into a "modified Fourier series" with terms equal to the corresponding term of the Fourier series for linear motors with a winding of "infinite length", in the interval $2p\tau_p$ symmetrically covering the phase winding, and outside of it they are zero. (Poles number $2p$ that may be an odd number.) This "modified Fourier series" minimizes the mean square error integral for the finite excitation as does the Fourier series for the "infinite" excitation. All three phases of the winding fed by a symmetric, three-phase sine current system bring about for any (encountered) harmonic a finite standing wave of length $2p\tau_p$, all of them being decomposable into finite traveling waves of positive and negative order, again of length $2p\tau_p$. Taking the resultant of ν-th harmonic waves of the three phases, let us consider by the time the case $\nu=6k+1$. Indicating finite sinusoidal traveling waves by rectangles each, Figs 2a and b superpose traveling waves of positive and of negative order, respectively (belonging to different phases), whether there are waves of positive order, hence cophased, or of negative order, with phase lags of 120° but, not extincting each other at the edges. The case $\nu=6k-1$ differs from the former one merely by the prevalence of negative-order waves over those of positive order. Finally, for $\nu=3k$ phase lag between traveling waves of either positive or

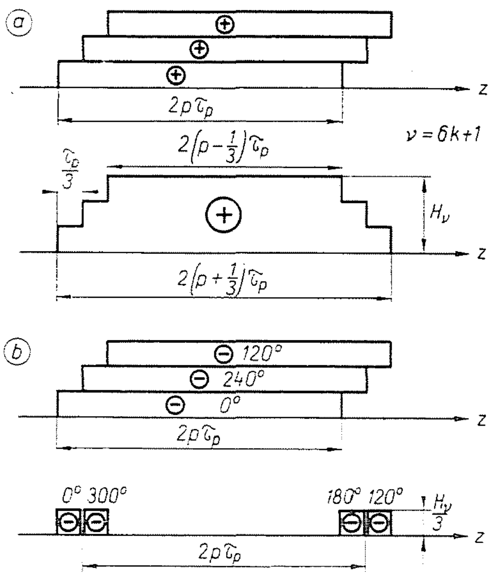

Fig. 2

negative order is 120°, so that finite traveling waves of either order are superposed as seen in Fig. 2b. These are negligible compared to traveling waves of fundamental harmonic (positive order), namely they arise only at winding extremities with amplitude $H_{3k}/3$, less than third of the H_1 value because of $\xi_{3k}<\xi_1$ according to Eqs (2) and (3), what is more, when fluxes are compared, division by $3k$ is imposed by the smaller wave length. The same is true for traveling waves of order $(6k\pm1)$ resulting at winding extremities except for the fundamental harmonic wave of negative order, it being of the same wave length, division is needless in comparing the fluxes. Finally, all traveling waves (even the stepped ones) of order $\nu\geqq 11$ may be neglected, namely for $\nu\geqq 11$,

$\xi_\nu \ll \xi_1$ (force and impedance will be seen below to be proportional to ξ_ν^2), furthermore comparison of fluxes requires division by a high number. In conclusion, nothing but the following traveling waves are worth being considered:

a) fundamental harmonic, positive order (stepped);
b) fundamental harmonic, negative order (at extremities alone);
c) fifth harmonic, negative order (stepped);
d) seventh harmonic, positive order (stepped).

Let us consider now the ease where parts of all phase windings inside one pole pitch have slots filled to the half at both extremities (the case of two-layer windings). Distribution H_z for one phase winding is half the value at edges of length τ_p of the interval of length $2p\tau_p$ than inside (rectangles being half as high). Applying a "modified Fourier series" where also the sine function sections of the terms at edges of length τ_p are half the amplitude as inside, while outside they are zero, the previously described method yields resultants of traveling waves of order $\nu = 6k+1$, of positive and negative order as seen in Fig. 3.

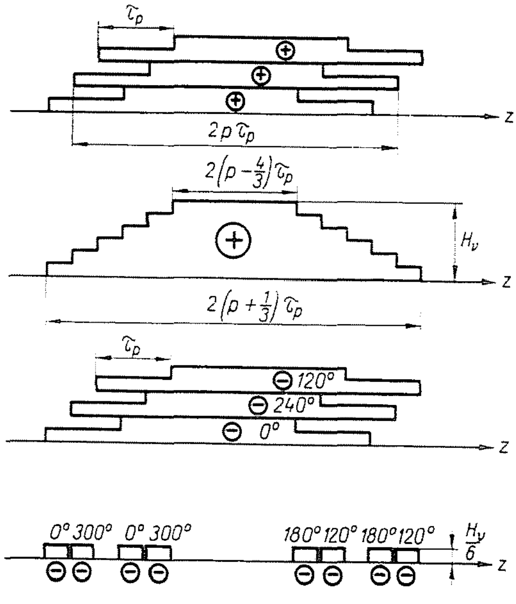

Fig. 3

Circumstances are seen to be similar to those for motors with fully filled slots, main differences being the step proportions and numbers.

In the case $\nu = 6k-1$ the negative-order wave is stepped, while the positive-order one arises at extremities alone. Case $\nu = 3k$ is irrelevant, yielding the same conslusions for traveling waves to be considered as for fully filled slots.

Stepped fundamental harmonic, fifth and seventh harmonic traveling waves of the tangential component of magnetic field intensity will be transformed by realizing the stepped configuration of distribution to be repeated within a certain — rather long — period, a distribution to be expanded into Fourier series, after having simplified the computation by replacing it by a trapezium with straight lines halving the steps at non-parallel sides, a substitution of slight error. Trapezium sizes for full windings, and for half-wound extremities are seen in Figs 4a and b, respectively. Denoting the

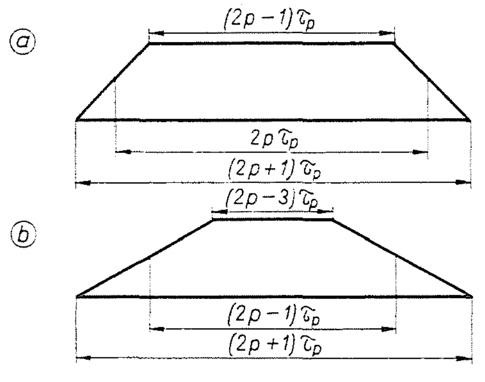

Fig. 4

shorter parallel trapezium side by $2z_1$, the longer one by $2z_2$, and the period length by $2z_p$, the three-term Fourier series of the trapezium function $T(z)$ of unit height becomes:

$$T_F(z)=a_0+a_1\cos\left(\frac{\pi}{z_p}z\right)+a_2\cos\left(\frac{2\pi}{z_p}z\right),$$

where

$$a_0=\frac{z_1+z_2}{2z_p},$$

$$a_1=\frac{4}{\pi}\frac{z_p}{z_2-z_1}\sin\left(\frac{z_2-z_1}{2z_p}\pi\right)\sin\left(\frac{z_2+z_1}{2z_p}\pi\right),$$

$$a_2=\frac{1}{\pi^2}\frac{z_p}{z_2-z_1}\sin\left(\frac{z_2-z_1}{z_p}\pi\right)\sin\left(\frac{z_2+z_1}{z_p}\pi\right).$$

The approximate function will be simplified by choosing z_p so that $a_2=0$. Meeting also the natural requirement $z_p>z_2$ yields:

$$z_p=z_1+z_2$$

From Fig. 4, obviously, for a fully wound machine:

$$2z_p\equiv 2z_1+2z_2=[(2p-1)\tau_p+(2p+1)\tau_p]=4p\tau_p,$$

and for one half wound at extremities:

$$2z_p\equiv 2z_1+2z_2=[(2p-3)\tau_p+(2p+1)\tau_p]=(4p-2)\tau_p.$$

Thus

$$z_p=2p_1\tau_p$$

where

$$p_1=\begin{cases} p & \text{(fully wound)} \\ p-\dfrac{1}{2} & \text{(half wound at extremities)} \end{cases} \tag{4}$$

The approximate function being:

$$T_F(z)=\frac{1}{2}+\frac{2}{\pi}\frac{\sin\alpha}{\alpha}\cos\left(\frac{\pi}{2p_1}\frac{z}{\tau_p}\right)$$

where

$$\alpha=\frac{z_2-z_1}{z_2+z_1}\frac{\pi}{2}$$

According to Fig. 4:

$$\alpha=\begin{cases} \dfrac{\pi}{4p} & \text{(fully wound)} \\ \dfrac{\pi}{2p-1} & \text{(half wound at extremities)} \end{cases} \tag{5}$$

In final account:

$$T_F(z)\cong 0.5+0.64\frac{\sin\alpha}{\alpha}\cos\left(\frac{\pi z}{2p_1\tau_p}\right) \tag{6}$$

Let us agree partly in Θ hence H_ν to indicate effective values in the following, giving for the complex instantaneous value of the uniformly distributed ν-th harmonic traveling wave·

$$\sqrt{2}H_\nu e^{j\left(\omega_0 t-\nu\frac{z}{\tau_p}\pi\right)}$$

and partly—in conformity with this latter statement— in marking the wave of positive or negative order by ν with a positive or negative sign [since according to (2), $\xi_{-\nu}=\xi_\nu$ this convention causes no trouble]. Thus, the complex instantaneous value of the νth harmonic traveling wave of trapezoidal distribution is:

$$H_{z\nu}^{(tr)}=\sqrt{2}H_\nu T(z)e^{j\left(\omega_0 t-\nu\frac{z}{\tau_p}\pi\right)}$$

or, replacing $T(z)$ by $T_F(z)$ according to (6):

$$H_{z\nu}^{(tr)}=\sqrt{2}\cdot 0{,}5H_\nu e^{j\left(\omega_0 t-\nu\frac{z}{\tau_p}\pi\right)}+$$

$$+\sqrt{2}\cdot 0{,}32H_\nu e^{j\left[\omega_0 t-\left(\nu-\frac{1}{2p_1}\right)\frac{z}{\tau_p}\pi\right]}+$$

$$+\sqrt{2}\cdot 0{,}32H_\nu e^{j\left[\omega_0 t-\left(\nu+\frac{1}{2p_1}\right)\frac{z}{\tau_p}\pi\right]}$$

Thus, the ν-th traveling wave of trapezoidal distribution is decomposed into νth, $\left(\nu-\frac{1}{2p_1}\right)$th and $\left(\nu+\frac{1}{2p_1}\right)$th harmonic traveling waves of uniform distribution, with effective values of $0{,}5H_\nu$; $0{,}32\frac{\sin\alpha}{\alpha}H_\nu$ and $0{,}32\frac{\sin\alpha}{\alpha}H_\nu$, respectively. It was seen above that from among traveling waves of trapezoidal distribution, only harmonics of orders $\nu=1$, $\nu=-5$, and $\nu=7$ merit to be reckoned with. Wave lengths

$$\frac{\tau_p}{5+\frac{1}{2p_1}} \quad \text{and} \quad \frac{\tau_p}{5-\frac{1}{2p_1}}$$

of uniformly distributed waves of orders $\left(-5-\frac{1}{2p_1}\right)$ and $\left(-5+\frac{1}{2p_1}\right)$ obtained by decomposing the fifth harmonic wave of trapezoidal distribution are practically symmetric about the fifth harmonic wave length $\tau_p/5$, with slight deviations, causing their influence on impedance and force to be averaged, hence it suffices to apply a single fifth harmonic of uniform distribution, of an effective value:

$$\left(0{,}5+0{,}64\frac{\sin\alpha}{\alpha}\right)\cdot H_5$$

This is still more valid for the seventh harmonic. For the fundamental harmonic, the arising evenly distributed traveling waves of orders

$$\nu=1, \qquad \nu=\left(1-\frac{1}{2p_1}\right) \qquad \text{and} \qquad \nu=\left(1+\frac{1}{2p_1}\right)$$

are, however, to be considered separately.

The fundamental harmonic traveling wave of negative order of non-trapezoidal distribution, arising only at extremities, will be replaced by its zeroth Fourier component, hence its mean value for the period length $4p_1\tau_p$, indicating for both winding types a wave of negative order, with a value 0, namely

$$e^{j0}+e^{j\frac{5\pi}{3}}+e^{j\pi}+e^{j\frac{2\pi}{3}}=0.$$

Thus, harmonic traveling waves of uniform distribution, to be reckoned with, are of the orders:

$$\nu=1, \quad 1-\frac{1}{2p_1}, \quad 1+\frac{1}{2p_1}, \quad -5, \quad 7, \quad -1; \tag{7}$$

with effective values according to Eq. (3):

$$H_{ze\nu}=b_\nu\frac{3\Theta q}{\tau_p} \tag{8}$$

where

$$\left.\begin{aligned} & b_1=0{,}5\xi_1 \\ & b_{1-\frac{1}{2p_1}}=b_{1+\frac{1}{2p_1}}=0{,}32\frac{\sin\alpha}{\alpha}\xi_1 \\ & b_{-5}=\left(0{,}5+0{,}64\frac{\sin\alpha}{\alpha}\right)\xi_5 \\ & b_7=\left(0{,}5+0{,}64\frac{\sin\alpha}{\alpha}\right)\xi_7 \\ & b_{-1}\approx 0. \end{aligned}\right\} \tag{9}$$

The p_1, α and ξ_ν values will be obtained from Eqs (4), (5) and (2), respectively.

3. Computation of the terminal impedance and the force

In knowledge of the slot excitation Θ, relationship (8) permits to determine the tangential component of the magnetic field intensity of every traveling harmonic wave to be taken into account along the boundary plane of the primary part of the double-sided linear motor shown in section in Fig. 5; a boundary plane has the co-ordinates $x = \pm\delta$ in the assumed co-ordinate system, therefore, considering the phase position of Θ to be real, for the phasor $\mathbf{H}_{z\nu}$ given with its effective value:

$$(\mathbf{H}_{z\nu})_{x=\pm\delta} = \pm H_{ze\nu} \,. \qquad (10)$$

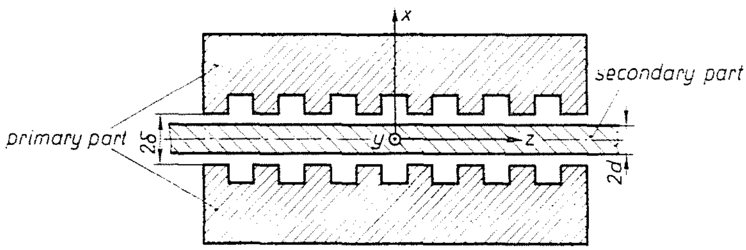

Fig. 5

Complex momentary value of the ν-th harmonic of the field characteristic being:

$$\sqrt{2}\mathbf{H}_{z\nu} e^{j\left(\omega t - \nu \frac{z}{\tau_p}\pi\right)}$$

by convention, field characteristic phasors do not contain the dependence on z either. In the coordinate system fitted to the primary part $\omega = \omega_0 = 2\pi f$, where f is the line frequency; in the co-ordinate system fitted to the secondary part $\omega = \omega_\nu$ where ω_ν is the circular frequency of the current induced by the ν-th harmonic field in the secondary part.

Velocity of the fundamental harmonic of the traveling field, compared to the primary part:

$$v_0 = \frac{\omega_0 \tau_p}{\pi} = 2f\tau_p \qquad (11)$$

and the slip in case of a secondary part traveling at velocity v along z, compared to the primary part:

$$s=\frac{v_0-v}{v} \tag{12}$$

The ν-th harmonic traveling field has a velocity v_0/ν compared to the primary part; its slip being:

$$s_\nu=\frac{\frac{v_0}{\nu}-v}{\frac{v_0}{\nu}}=1-\nu(1-s) \tag{13}$$

hence the circular frequency of the current in the secondary part (due to the ν-th harmonic):

$$\omega_\nu=s_\nu\omega_0=[1-\nu(1-s)]\omega_0 \tag{14}$$

For a linear motor of infinite width (in direction y), among field characteristic components only H_z, H_x and $E_y=E$ are non-zero and they are independent of y.

Hence phasors $\mathbf{H}_{z\nu}$, $\mathbf{H}_{x\nu}$, $\mathbf{E}_\nu$ depend only on x. Substituting the complex momentary values into the Maxwell equations, in the co-ordinate system fitted to the secondary part, phasors will be expressed by the following ordinary differential equation system:

$$-j\nu\frac{\pi}{\tau_p}\mathbf{H}_{x\nu}-\frac{d\mathbf{H}_{x\nu}}{dx}=\gamma\mathbf{E}_\nu \tag{15a}$$

$$\frac{d\mathbf{E}_\nu}{dx}=-j\omega_\nu\mu_0\mathbf{H}_{z\nu} \tag{15b}$$

$$j\nu\frac{\pi}{\tau_p}\mathbf{E}_\nu=-j\omega_\nu\mu_0\mathbf{H}_{x\nu} \tag{15c}$$

where γ is the conductivity of the non-ferromagnetic secondary part. For positive x values, E and $-H_z$ yield power flow toward the secondary part.

Accordingly, the field impedance to be interpreted will be:

$$-\frac{\mathbf{E}}{\mathbf{H}_{zv}}$$

advisably converted to the primary part, taking into consideration that the electric field intensity is transformed into the primary one by the factor $\frac{\omega_0}{\omega_v}$, $\mathbf{H}_z$ being (practically) invariable. Hence, field impedance referred to the primary part:

$$\mathbf{Z}_v = -\frac{\omega_0}{\omega_v}\frac{\mathbf{E}_v}{\mathbf{H}_{zv}} \tag{16}$$

Re-writing differential equations (15) accordingly, yields:

$$\frac{d\mathbf{Z}_v}{dx} = j\omega_0\mu_0 + j\frac{\pi^2}{\tau_p^2}\frac{v^2}{\omega_0\mu_0}(1+jm_v)\mathbf{Z}_v^2$$

where

$$m_v = \frac{\gamma\mu_0\tau_p^2\omega_v}{\pi^2 v^2} \tag{17}$$

General solution of the differential equation for $\mathbf{Z}_v$:

$$\mathbf{Z}_v = \frac{\tau_p\omega_0\mu_0}{v\pi\sqrt{1+jm_v}}\,\mathrm{tg}\left(j\frac{\pi v x}{\tau_p}\sqrt{1+jm_v}+\mathbf{C}\right) \tag{18}$$

Because of symmetry, for the secondary part:

$$\text{for}\quad x=0,\qquad \mathbf{H}_{zv}=\mathbf{0},\qquad Z_v\to\infty$$

corresponding to $\mathbf{C}=\frac{\pi}{2}$; substituting $x=d$, the total field impedance of the secondary half-part becomes:

$$\mathbf{Z}_{v2}^{\infty} = \frac{\tau_p\omega_0\mu_0}{\pi v}\mathbf{k}_v^{\infty} \tag{19}$$

where

$$\mathbf{k}_\nu^\infty = \frac{1}{\sqrt{1+jm_\nu}\ \mathrm{tg}\left(-j\dfrac{\pi\nu d}{\tau_p}\sqrt{1+jm_\nu}\right)} \tag{20}$$

(superscript ∞ refers to the linear motor of infinite width).

The air gap field impedance will be obtained from (18) by substituting $\gamma=0$, hence from (17), substituting $m_\nu=0$:

$$\mathbf{Z}_{\nu a}^\infty = \frac{\tau_p\omega_0\mu_0}{\nu\pi}\ \mathrm{tg}\left(j\frac{\pi\nu x}{\tau_p}+\mathbf{C}_1\right);$$

because of the continuous transition of the field impedance:

$$(\mathbf{Z}_{\nu a}^\infty)_{x=d} = \mathbf{Z}_{\nu 2}^\infty$$

hence:

$$\mathrm{tg}\left(j\frac{\pi\nu d}{\tau_p}+\mathbf{C}_1\right) = \mathbf{k}_\nu^\infty$$

Field impedance taking also the air gap effect into consideration, related to the voltage induced in the winding, along the boundary plane of the primary part, at $x=\delta$:

$$\mathbf{Z}_{\nu i}^\infty = (\mathbf{Z}_{\nu a}^\infty)_{x=\delta} = \frac{\tau_p\omega_0\mu_0}{\nu\pi}\ \mathrm{tg}\left(j\frac{\pi\nu\delta}{\tau_p}+\mathbf{C}_1\right)$$

eliminating C_1:

$$\mathbf{Z}_{\nu i}^\infty = \frac{\tau_p\omega_0\mu_0}{\nu\pi}\ \mathbf{K}_\nu^\infty, \tag{21}$$

and

$$\mathbf{K}_\nu^\infty = \frac{\mathbf{k}_\nu^\infty + j\tanh\left[\dfrac{\pi\nu}{\tau_p}(\delta-d)\right]}{1-j\,\mathbf{k}_\nu^\infty\tanh\left[\dfrac{\pi\nu}{\tau_p}(\delta-d)\right]} \tag{22}$$

In discussing linear motors of finite width, it is normally taken into consideration that the secondary part is generally wider than the primary part to keep the bend of eddy current flows apart from the iron core conducting most of the primary flux (Fig. 6).

In the part of the secondary plate overhanging the iron core, voltages induced by the winding head flux and the dependence on x of the field characteristics will be ignored, yielding for the components of potential electric field intensity in the domains

$$\frac{1}{2}l \leqq |y| \leqq \frac{1}{2}(l+l_s),$$

$$\mathbf{E}_{y\nu} = -\frac{d\mathbf{V}_\nu}{dy}, \quad \mathbf{E}_{z\nu} = -j\frac{\pi}{\tau_p}\nu\mathbf{V}_\nu, \quad \mathbf{E}_{x\nu} = \mathbf{0},$$

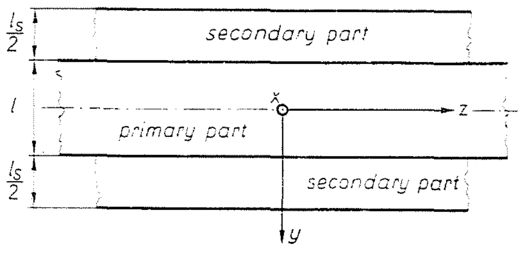

Fig. 6

where $\mathbf{V}_\nu$ is the potential phasor in the ν-th harmonic traveling field. Since no current can leave across the edge of the secondary plate,

$$(\mathbf{E}_{y\nu})_{|y|=\frac{l+l_s}{2}} = \left(-\frac{d\mathbf{V}_\nu}{dy}\right)_{|y|=\frac{l+l_s}{2}} = \mathbf{0}$$

Solution of the Laplace equation for $\mathbf{V}_\nu$ meeting this boundary condition is:

$$\mathbf{V}_\nu = \mathbf{V}_{0\nu}\left[e^{\frac{\pi\nu}{\tau_p}|y|} + e^{\frac{\pi\nu}{\tau_p}(l+l_s-|y|)}\right]$$

yielding the prescription for the inner domain edges:

$$\left(\frac{\mathbf{E}_{y\nu}}{\mathbf{E}_{z\nu}}\right)_{|y|=\frac{l}{2}} \equiv \left(j\frac{\tau_p}{\pi\nu}\frac{d\mathbf{V}_\nu}{dy}\frac{1}{\mathbf{V}_\nu}\right)_{|y|=\frac{l}{2}} = -j\kappa \operatorname{sgn}(y) \tag{23}$$

$$\kappa = \frac{e^{\frac{\pi}{\tau_p}\nu l_s} - 1}{e^{\frac{\pi}{\tau_p}\nu l_s} + 1} \equiv \tanh\left(\frac{\pi\nu l_s}{2\tau_p}\right) \tag{24}$$

The electromagnetic field in the part of the secondary plate below the iron core is considered to consist of two parts. One is the field with phasors $\mathbf{H}_{x\nu}$, $\mathbf{H}_{z\nu}$ and $\mathbf{E}_\nu$ discussed in connection with the linear motor of infinite width, the other being a correction electromagnetic field containing component phasors $\mathbf{E}'_{y\nu}$, $\mathbf{E}'_{z\nu}$ and $\mathbf{H}'_{x\nu}$, thus:

$$\left.\begin{aligned}\mathbf{E}_{y\nu}&=\mathbf{E}_\nu+\mathbf{E}'_{y\nu}\\ \mathbf{E}_{z\nu}&=\mathbf{E}'_{z\nu}\end{aligned}\right\} \tag{25}$$

Correction field characteristics are considered (with an approximation) to be independent of x, and replacing them into the Maxwell equations yields the system of differential equations

$$-j\frac{\pi}{\tau_p}\nu\mathbf{H}'_{x\nu}=\gamma\mathbf{E}'_{y\nu},$$

$$-\frac{d\mathbf{H}'_{x\nu}}{dy}=\gamma\mathbf{E}'_{z\nu},$$

$$\frac{d\mathbf{E}'_{z\nu}}{dy}+j\frac{\pi}{\tau_p}\nu\mathbf{E}'_{y\nu}=-j\omega_\nu\mu_0\mathbf{H}'_{x\nu}$$

eliminating $\mathbf{H}_{x\nu}$ and applying notations in (17) yields the system of differential equations

$$\frac{d\mathbf{E}'_{y\nu}}{dy}=j\frac{\pi}{\tau_p}\nu\mathbf{E}'_{z\nu}, \tag{26a}$$

$$\frac{d\mathbf{E}'_{z\nu}}{dy}=-j\frac{\pi}{\tau_p}\nu(1+jm_\nu)\,\mathbf{E}'_{y\nu}. \tag{26b}$$

Symmetry requires $\mathbf{E}'_{z\nu}$ to be an odd function, giving the solution for (26):

$$\mathbf{E}'_{z\nu}=\mathbf{E}_0\sinh\left(\frac{\pi}{\tau_p}\nu\sqrt{1+\mathrm{j}m_\nu}\,y\right) \tag{27a}$$

$$\mathbf{E}'_{y\nu}=j\frac{\mathbf{E}_0}{\sqrt{1+jm_\nu}}\cosh\left(\frac{\pi\nu}{\tau_p}\sqrt{1+\mathrm{j}m_\nu}\,y\right) \tag{27b}$$

To determine $\mathbf{E}_0$, relationships (23), (25) and (27) will be confronted.

In (25), $\mathbf{E}_\nu$ depends on x, so that (23) can only be met by a mean value along x. Introducing notation

$$\mathbf{E}_\nu^m = \frac{1}{d} \int_0^d \mathbf{E}_\nu dx \tag{28}$$

yields

$$\mathbf{E}_0 = \frac{j\sqrt{1+jm_\nu}\,\mathbf{E}_\nu^m}{\kappa\sqrt{1+jm_\nu}\,\sinh \mathbf{a} + \cosh \mathbf{a}} \tag{29}$$

where

$$\mathbf{a} = \nu \frac{\pi l}{2\tau_p} \sqrt{1+jm_\nu} \tag{30}$$

Calculation of the correction impedance needs the mean value of $\mathbf{E}'_{y\nu}$ along y modifying the $\mathbf{E}_\nu$ value; thereby, using interpretation (16), correction field impedance of the secondary part becomes:

$$\mathbf{Z}'_{\nu 2} = -\frac{\omega_0}{\omega_\nu} \frac{\frac{2}{l}\int_0^{l/2} \mathbf{E}'_{y\nu} dy}{(\mathbf{H}_{z\nu})_{x=d}}$$

($\mathbf{E}'_{z\nu}$ with $\mathbf{H}_{z\nu}$ yielding no power)
Considering relationships

$$\frac{d\mathbf{H}_{z\nu}}{dx} = j\frac{\gamma}{m_\nu}(1+jm_\nu)\mathbf{E}_\nu$$

obtained from (15a,c) using notation (17) and

$$(\mathbf{H}_{z\nu})_{x=d} = \frac{\gamma d}{m_\nu} j(1+jm_\nu)\mathbf{E}_\nu^m$$

obtained from it using notation (28) and equation $(\mathbf{H}_{z\nu})_{x=0} = \mathbf{0}$ as well as Eq. (26b) and notation (17):

$$\mathbf{Z}'_{\nu 2} = -\frac{2}{ld} \frac{\omega_0 \mu_0 \tau_p^3}{\pi^3 \nu^3} \frac{1}{(1+jm_\nu)^2} \frac{(\mathbf{E}'_{z\nu})_{y=\frac{l}{2}}}{\mathbf{E}_\nu^m}$$

Finally, taking Eqs (27a), (29) and notation (30) into consideration:

$$\mathbf{Z}'_{\nu 2} = -\frac{\tau_p \omega_0 \mu_0}{\pi \nu} \mathbf{k}'_\nu \tag{31}$$

where

$$\mathbf{k}'_\nu = \frac{j \dfrac{2\tau_p^2}{\pi^2 \nu^2 ld}}{(1 + jm_\nu)[\kappa(1 + jm_\nu) + \sqrt{1 + jm_\nu} \coth \mathbf{a}]} \tag{32}$$

Thus, the secondary field impedance referred to the primary part, modified by a correction term (for the ν-th harmonic):

$$\mathbf{Z}_{\nu 2} = \mathbf{Z}_{\nu 2}^{\infty} + \mathbf{Z}'_{\nu 2} \, .$$

Taking (19) and (31) into consideration:

$$\mathbf{Z}_{\nu 2} = \frac{\tau_p \omega_0 \mu_0}{\pi \nu} \mathbf{k}_\nu \tag{33}$$

where

$$\mathbf{k}_\nu = \mathbf{k}_\nu^{\infty} - \mathbf{k}'_\nu \tag{34}$$

Remark that this computation method of the transversal edge effect due to the finite machine width is essentially the Bolton model [4] adapted to this computation method. Thereby the skin effect and the transversal edge effect can simultaneously be taken into consideration, with the approximation that the correction of the transversal end effect does not contain the skin effect, furthermore, the transversal edge effect can be reckoned with for every harmonic, permitting correct handling of the co-existence of longitudinal and transversal end effects. Because of the finite width, magnetic flux leaves the air gap also along y, omitted for the two-dimensional model of the linear motor of infinite width. Computing the ν-th harmonic of the potential magnetic field of the air gap using a three-dimensional model:

$$\mathbf{H}_{x\nu} = -\frac{\partial \mathbf{W}_\nu}{\partial x}, \qquad \mathbf{H}_{y\nu} = -\frac{\partial \mathbf{W}_\nu}{\partial y}, \qquad \mathbf{H}_{z\nu} = j\frac{\pi}{\tau_p} \nu \mathbf{W}_\nu$$

where $\mathbf{W}_\nu$ is the potential phasor. The Laplace equation being valid for $\mathbf{W}_\nu$:

$$\frac{\partial^2 \mathbf{W}_\nu}{\partial x^2} + \frac{\partial^2 \mathbf{W}_\nu}{\partial y^2} - \frac{\pi^2}{\tau_p^2} \nu^2 \mathbf{W}_\nu = \mathbf{0}$$

Replacing the rectangular relative flux distribution along y seen in Fig. 7 by a function $1{,}17\cos\left(2{,}34\frac{y}{1}\right)$, of the same area (flux) as the rectangle, approximating it with a minimum mean square error, then the Laplace equation will be met with respect to y by the distribution y:

$$\mathbf{W}_v=\mathbf{W}_{v1}\cdot 1{,}17\cos\left(2{,}34\frac{y}{l}\right),$$

yielding the following two-dimensional Laplace equation:

$$\frac{d^2\mathbf{W}_{v1}}{dx^2}-\left[\left(\frac{2{,}34}{l}\right)^2+\frac{\pi^2v^2}{\tau_p^2}\right]\mathbf{W}_{v1}=\mathbf{0}$$

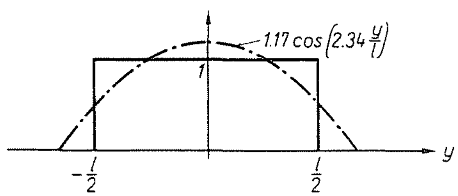

Fig. 7

The same equation results from the two-dimensional model for $l\to\infty$ if the τ_p value is changed into τ_p/β in order to obtain:

$$\frac{\pi^2v^2}{\tau_p^2}\beta^2=\left(\frac{2{,}34}{l}\right)^2+\frac{\pi^2v^2}{\tau_p^2}$$

thus:

$$\beta=\sqrt{1+0{,}554\frac{\tau_p^2}{l^2v^2}} \tag{35}$$

Thereby τ_p replaced by τ_p/β in (22), approximating the effect of the finite width on the air gap; of course $\mathbf{k}_v^\infty$ in (22) will be replaced by $\mathbf{k}_v$, thus, according to (21)

$$\mathbf{Z}_{vi}=\frac{\tau_p\omega_0\mu_0}{v\pi}\mathbf{K}_v \tag{36}$$

and

$$\mathbf{K}_\nu = \frac{\mathbf{k}_\nu + j\tanh\left[\beta\frac{\pi\nu}{\tau_p}(\delta-d)\right]}{1-j\mathbf{k}_\nu\tanh\left[\beta\frac{\pi\nu}{\tau_p}(\delta-d)\right]} \tag{37}$$

Field impedance $\mathbf{Z}_{\nu i}$ is valid at $x=\delta$, boundary plane of the primary part; at the same place the electric field intensity in the co-ordinate system fitted to the primary part, using (10):

$$(\mathbf{E}_\nu^p)_{x=\delta} = -(\mathbf{H}_{z\nu})_{x=\delta}\mathbf{Z}_{\nu i} = -H_{ze\nu}\mathbf{Z}_{\nu i}$$

spatial mean voltage induced in a lead of the winding of slot-opening c by the ν-th harmonic wave being for $q=1$, and in case of a primary iron core of width l:

$$\mathbf{U}_{\nu i} = l\frac{1}{c}\int_{-\frac{c}{2}}^{\frac{c}{2}}(-\mathbf{E}_\nu^p)_{x=\delta}e^{-j\frac{\pi}{\tau_p}z}dz =$$

$$= lH_{ze\nu}\mathbf{Z}_{\nu i}\frac{\sin\left(\nu\frac{c}{\tau_p}\frac{\pi}{2}\right)}{\nu\frac{c}{\tau_p}\frac{\pi}{2}}$$

For $q \neq 1$, it has to be multiplied by the chord factor

$$\frac{\sin\left(\nu\frac{\pi}{6}\right)}{q\sin\left(\nu\frac{\pi}{6q}\right)}$$

hence, using notation (2), formulae (8) and (36):

$$\mathbf{U}_{\nu i} = lH_{ze\nu}\xi_\nu\mathbf{Z}_{\nu i} = \frac{3}{\pi}ql\omega_0\mu_0\frac{b_\nu\xi_\nu}{\nu}\Theta\mathbf{K}_\nu.$$

Remark, however, that for a traveling harmonic wave of fraction order, the motor winding is other than diametral. Therefore the ξ_ν value has to be multiplied by a winding factor taking this fact into consideration, modifying formula (2) to:

$$\xi_\nu = \frac{\sin\left(\nu \frac{\pi}{\tau_p}\frac{c}{2}\right)}{\nu \frac{\pi}{\tau_p}\frac{c}{2}} \cdot \frac{\sin\left(\nu \frac{\pi}{6}\right)}{q \sin\left(\nu \frac{\pi}{6q}\right)} \cdot \xi'_\nu ,$$

$$\xi'_\nu = \frac{\sin\left[p_1 (\nu-1)\pi\right]}{2p_1 \sin\left[\frac{(\nu-1)\pi}{2}\right]} \cdot \cos\left[\frac{\pi(p-p_1)}{2p_1}\right]. \tag{2*}$$

[The last factor yields for odd ν values 0/0 to be taken as unity; it gives a value less than 1 only for $\nu = 1 \pm \frac{1}{2p_1}$; so right-hand sides of Eqs (9) are inaffected by modification (2*).] For traveling waves of fraction order, also phase-shift of voltages induced in the phase windings slightly differ from 120°, resulting also in voltages of negative order. For the two waves of fraction order, however, deviations from 120° are offset opposite to each other, permitting to neglect this effect. Among all the considered harmonic fields, only the $\nu = -1$-th one is considered to induce voltages of negative order; hence, all the induced voltages of positive order are:

$$\mathbf{U}_i^+ = \frac{3}{\pi} q l \omega_0 \mu_0 \Theta \sum_{\nu;\nu \neq -1} \frac{b_\nu \xi_\nu}{\nu} \mathbf{K}_\nu$$

and those of negative order:

$$\mathbf{U}_1^- = -\frac{3}{\pi} q l \omega_0 \mu_0 \Theta \; {}_{-1}\xi_{-1} \mathbf{K}_{-1} \approx \mathbf{0},$$

both being due to excitation of positive order. Accordingly, the impedance referring to a slot, interpreted as

$$\mathbf{Z}_i = \frac{\mathbf{U}_i^+}{\Theta} = \frac{3}{\pi} q l \omega_0 \mu_0 \sum_\nu \frac{b_\nu \xi_\nu}{\nu} \mathbf{K}_\nu . \tag{38}$$

(Factor ξ_ν^2 referred to in Chapter 2 appears now in Eq. (38) based on (9) in the case $\nu \geqq 5$). Neglecting the excitation share of teeth and core, excitation Θ for the slot equals the total slot current, and winding resistance as well as slot and winding overhang leakage reactance for a slot are connected in series with the internal impedance Z_i. Terminal impedance for a slot becomes:

$$\mathbf{Z} = R + jX_l + \mathbf{Z}_i \tag{39}$$

Notice that in possession of these results, determination of the tooth induction, and from it, knowing the magnetization curve, the excitation excess $\Delta\Theta$ is not difficult, yielding for the current flowing through the impedance $R+jX_l$:

$$\Theta_1 = \Theta + \Delta\Theta$$

not to be treated in detail.

For determining the thrust of linear induction motors, let us mention first that equations of the considered harmonic traveling waves constitute an orthogonal function system; namely repetition interval $4p_1\tau_p$ is integer multiple of the period length of harmonics of fraction order too, namely:

$$4p_1\tau_p : \frac{2\tau_p}{1 \pm \frac{1}{2p_1}} = 2p_1 \pm 1$$

an integer number according to (4).

Thus, interaction between harmonics of different orders results in no power or force.

Air gap power of the ν-th harmonic wave equals the effective power on the internal impedance, thus, according to (38):

$$P_{a\nu} = \frac{3}{\pi} ql\omega_0\mu_0 \frac{b_\nu\xi_\nu}{\nu} \Theta^2 Re(\mathbf{K}_\nu)$$

Travel velocity of the same field being, from (11):

$$\frac{v_0}{\nu} = \frac{\omega_0\tau_p}{\pi\nu}$$

with a thrust

$$F_\nu = P_{a\nu} \frac{\pi\nu}{\omega_0\tau_p}$$

and the total thrust for a slot:

$$F = 3q \frac{l}{\tau_p} \mu_0\Theta^2 \sum_\nu b_\nu\xi_\nu Re(\mathbf{K}_\nu) \tag{40}$$

On the other side of the double-sided linear motor, the same impedance and force result for each slot. Computation needs the following formulate, in that order:

(7), (14), (17), (20), (24), (30), (32), (34), (37), (2*), (4), (5), (9), (38), (39), (40).

Remark that impedance Z_i is serial resultant of impedances belonging to each harmonic wave; for each impedance an equivalent circuit analogous to the rotating induction motor can be constructed; to be find in [16] for the fundamental harmonic.

Summary

Tangential component of the magnetic field intensity along the boundary plane of the primary part of a linear induction motor is approximated by six undamped traveling harmonic waves, two of them being of fraction order compared to the fundamental harmonic datermined by pole division. For all traveling waves, an impedance taking (approximately) the effect of finite width into consideration is defined: the motor impedance is their resultant. The algorithm is concluded by calculating the force.

References

1. LAITHWAITE, E. R.: The goodness of a machine. PROC. IEE. Vol. 112. No 3. MARCH 1965; 538—541
2. FREEMAN, E. M.: Travelling waves in induction machines: input impedance and equivalent circuits. PROC. IEE, Vol. 115, No. 12, DECEMBER 1968;1772—1776.
3. NASAR, S. A.: Electromagnetic fields and forces in a linear induction motor, taking into account edge effects. PROC. IEE, Vol. 116. No. 4. APRIL 1969; 605—609.
4. BOLTON, H. R.: Transverse edge effect in sheet-rotor induction motors. PROC. IEE, Vol. 116. No. 5. MAY 1969; 725—731.
5. VOLDEK, A. J.—LAZARENKO, L. F.: Prodolnye kraevye effekti v lineynikh induktzionnikh magnitogidrodinamitcheskikh mashinakh. Elektritchestvo No. 11. 1970; 26—30.
6. POLOUJADOFF, M.—REYX, PH.: Méthode intermédiaire pour l'analyse d'un moteur ā induction linéaire. R. G. E. — Tome 80 No. 2 Février 1971, 99—104.
7. YAMAMURA, S.—ITO, H.—ISHIKAWA, Y.: Theories of the linear induction motor and compensated linear induction motor. IEEE Winter Meeting, New York, January 30—February 4, 1972, Paper T 72 060—7.
8. KAPCSOS, P.—TEVAN, GY.: Application and Computation of Linear Eddy Current Motors with Ferromagnetic Core*. Elektrotechnika 65. 1972. No. 12. 458—465.
9. SCHIBER, D.: Principles of Operation of Linear Induction Devices. Proceeding of the IEEE, Vol. 61, No. 5, May 1973; 647—656.
10. OBERRETL, K.: Dreidimensionale Berechnung des Linearmotors mit Berücksichtigung der Endeffekte und der Wicklungsverteilung. Archiv für Elektrotechnik. Bd. 55, H. 4 (1973), 181—190.
11. BOON-TECK OOI: A Generalized Machine Theory of the Linear Induction Motor. IEEE Winter Meeting, New York, January 28—February 2, 1973; 1252—1259.
12. AGARWAL, P. D.—WANG, T. C.: Evaluation of Fixed and Moving Primary Linear Induction Motor System. Proceedings of the IEEE, Vol. 61, 1973. No. 5.
13. ALDEN, R. T. H.—NOLAN, P. J.: Transfer-Matrix Analysis of Linear Induction Machines with Finite Width and Depth. Proc. IEE, Vol. 121, No. 11, November, 1974, 1393—1398.

14. VOLDEK, A. I.—TOLVINSKAYA, E. B.: Osnovi teorii metodiki rastchota kharakteristik lineynikh asinkronnikh mashin. Elektritchestvo No. 9, 1975, 29—36.
15. SAKAE YAMAMURA: Theory of Linear Induction Motors. John Wiley and sons. New York—London—Sydney—Toronto, 1972.
16. TEVAN, GY.—TÓTH F.: A Clear Algorithm for the Calculation of the Linear Induction Motor Based on Field Theory. Acta Technica Academiae Scientiarum Hungaricae 86, 3—4 (1978).
17. YAMAMURA, S.—ITO, H.: Three-Dimensional Analysis of Linear Induction Motors. Electrical Engineering in Japan, Vol. 96, No. 2, 1976.
18. SCHIEBER, D.: Electrodynamics of Distributed-Parameter Induction Devices. Archiv für Elektrotechnik 59 (1977) 297—303.

* In Hungarian

Dr. György TEVAN, H-1521 Budapest